Journal of Molecular Spectroscopy 256 (2009) 80–85

Contents lists available at ScienceDirect

Journal of Molecular Spectroscopy

journal homepage: www.elsevier.com/locate/jms

On the ultraviolet absorption of nitrous oxide and its van der Waals complexes

Christof Maul [a,*], Mikhail Poretskiy [b], Asylkhan Rakhymzhan [c], Jörg Grunenberg [d]

[a] Institut für Physikalische und Theoretische Chemie, Technische Universität Braunschweig, Hans-Sommer-Straße 10, D-38106 Braunschweig, Germany
[b] St. Petersburg University, St. Petersburg, Russia
[c] Institute of Chemical Kinetics and Combustion, Novosibirsk, Russia
[d] Institut für Organische Chemie, Technische Universität Braunschweig, Braunschweig, Germany

ARTICLE INFO

Article history:
Received 31 December 2008
In revised form 9 February 2009
Available online 24 February 2009

Keywords:
Nitrous oxide
van der Waals complex
Rydberg state
Resonance enhanced multi-photon ionization (REMPI)
Density functional theory (DFT)

ABSTRACT

The possibility of simultaneous characterization of N_2O and N_2O van der Waals complexes in supersonic jet expansions is demonstrated for neat N_2O samples. Room temperature and jet-cooled spectra of the Rydberg transitions $3p\pi\,^1\Delta \leftarrow\leftarrow X\,^1\Sigma^+$ and $3p\sigma\,^1\Pi \leftarrow\leftarrow X\,^1\Sigma^+$ are presented. Theoretical calculations support the assignment of the Rydberg transitions used. For stagnation pressures above 2 bar, a hitherto unreported broad spectral feature at 84650 cm^{-1} is observed, where calculations predict absorption of the $(N_2O)_2$ dimer essentially due to excitation of the 4sσ and 3pπ Rydberg orbitals. Consequences for the use of N_2O as a precursor for $O(^1D)$ atoms in reactive scattering experiments are discussed.

1. Introduction

The important role of nitrous oxide (N_2O) in atmospheric chemistry [1,2] has motivated a large number of investigations of this molecule. It is not only an important greenhouse gas itself [3], but, upon irradiation with ultraviolet light, is also a primary source of excited $O(^1D)$ atoms [4] which are involved in the catalytic destruction of ozone via the reaction

$$O(^1D) + N_2O \rightarrow 2NO. \quad (1)$$

Additionally the nitrous oxide (N_2O) molecule is of interest from a fundamental point of view for at least two reasons. First, its dimer was one of the first van der Waals complexes investigated in a supersonic jet expansion [5], and second, it has widely been used as precursor molecule for $O(^1D)$ atoms, in particular for investigating the bimolecular reaction (1) which can be initiated with relative experimental ease by 193 nm laser radiation in a N_2O sample [6–20]. Frequently, such experiments are performed in supersonic expansions where low temperature and high number density favor the formation of N_2O van der Waals complexes which are likely to affect the course of the reaction [7,8,19,20].

The N_2O absorption spectrum has been studied by several groups [21–29]. It consists of a structured continuum ($B\,^1\Delta$) from 160 to 220 nm, diffuse bands from 140 to 160 nm ($C\,^1\Pi$), a dissociative continuum from 120 to 140 nm ($D\,^1\Sigma^+$), and a region of many Rydberg states from 100 to 120 nm. Whereas several theoretical calculations of the absorption spectrum have been performed for low energy excitation [30 and references therein], calculated spectra for the Rydberg region below 120 nm remain scarce [24,31].

The formation of N_2O complexes has previously been investigated by mass spectroscopy and by infrared spectroscopy, but has not yet been detected in the ultraviolet. It is well known that van der Waals complexes are formed in the free jet expansion of neat N_2O [32–41]. If the nozzle is pre-cooled and large stagnation pressures are applied, exclusively large clusters with up to several thousand molecules are observed, whereas for moderate expansion conditions smaller clusters prevail [32,33]. Specifically, the N_2O dimer has received and continues to receive considerable attention, in particular in infrared spectroscopy [34–41].

State selective excitation and detection of N_2O is possible by (2 + 1) resonance enhanced multi-photon ionization (REMPI) spectroscopy through its Rydberg states on the blue side of the $D\,^1\Sigma^+$ state. Only few such experimental studies [42–44] have been published up to date, mainly relying on a (3 + 1)-REMPI scheme in the wavelength range from 350 to 370 nm. Data on (2 + 1)-REMPI excitation are less abundant and exist only for few wavelength ranges and temperatures. Rydberg states are very well suited for detecting van der Waals complexes because they are significantly affected by the presence of another particle due to the large values of Rydberg radii [45,46]. Nevertheless, no REMPI data have yet been reported for N_2O van der Waals complexes.

Given the known Rydberg detection scheme of N_2O, the large sensitivity of Rydberg states towards complex formation, and the

* Corresponding author. Fax: +49 531 3915396.
E-mail address: c.maul@tu-bs.de (C. Maul).

0022-2852/$ - see front matter © 2009 Elsevier Inc. All rights reserved.
doi:10.1016/j.jms.2009.02.014

ease of complex generation of N_2O in a free jet expansion, the motivation for the presented work is to explore the possibility of simultaneous characterization of N_2O and N_2O van der Waals complexes in supersonic jet expansions which will not only allow one to characterize the composition of jet-cooled N_2O samples, but also promises to provide a tool for the characterization of Rydberg states of N_2O. In order to allow an assignment of the experimental results theoretical calculations have been performed on the absorption spectra of the isolated nitrous oxide molecule and the corresponding $(N_2O)_2$ dimer.

2. Experimental and theoretical methods

All calculations were performed using the Gaussian03 program package [47]. Ground state geometries for the N_2O monomer and the $(N_2O)_2$ dimer were optimized by second order Møller-Plesset perturbation theory (MP2). Excited state wavefunctions and vertical excitation energies were calculated by time-dependent density functional theory (TDDFT) using B3LYP, M052X, and MPW1PW91 functionals.

The experimental setup is described in detail in Ref. [48]. Basically, it consists of a home-built single-field time-of-flight (TOF) spectrometer with a total length of 0.57 m and a ratio of the acceleration region to the drift region of 1:2 which could be evacuated to a base pressure of 10^{-4} Pa. For room temperature experiments, pure N_2O was fed into the spectrometer via a needle valve resulting in typical sample pressures of 10^{-2} Pa. For low temperature experiments, pure N_2O was introduced via a free supersonic jet expansion onto the axis of the TOF spectrometer by a pulsed valve (General Valve Series 9). The diameter of the orifice was 0.5 mm, and stagnation pressures were varied from 1 to 8 bar. State-selective detection of N_2O was performed on fragment masses 30 (NO^+) and 28 (N_2^+) using an excimer laser pumped dye laser (Lambda Physik LPX 120i/LPD 3000) operated with Coumarin 102. The laser light was frequency doubled by a BBO crystal and focused into the spectrometer by a 60 mm quartz lens. The pulse energy was typically kept at 300 μJ. Ions were detected by a double stage multi-channel plate assembly with 40 mm active diameter. The ion signal was monitored, digitized, and integrated by a digital oscilloscope (LeCroy Waverunner) and stored by a personal computer. Alternatively, a combination of a digital oscilloscope (LeCroy 9450), a boxcar averager (Stanford Research), and an analog to digital converter was employed for the signal monitoring.

3. Theoretical results

N_2O in its electronic ground state is a closed shell linear molecule with $^1\Sigma^+$ configuration. Occupied orbitals are $[1\sigma^2 2\sigma^2 3\sigma^2 4\sigma^2 5\sigma^2 6\sigma^2]1\pi^4 7\sigma^2 2\pi^4$. Lowest unoccupied orbitals are $3\pi 8\sigma 9\sigma 4\pi$. The $(N_2O)_2$ dimer configuration with the lowest energy is known to be of anti-parallel slipped geometry with C_{2h} symmetry [40]. Its valence electronic configuration is $[...]7a_g^2 1a_u^2 1b_g^2 7b_u^2 8b_u^2 8a_g^2 9b_u^2 2b_g^2 9a_g^2 2a_u^2$, with lowest unoccupied orbitals $10b_u 3a_u 3b_g 10a_g 11a_g 11b_u 12b_u 4_u 12a_g 13a_g 4b_g 13b_u$. Due to the symmetry of the dimer and the weak, non-covalent interaction, the occupied dimer orbitals ($8b_u^2 8a_g^2$) and ($9b_u^2 2b_g^2 9a_g^2 2a_u^2$) essentially relate to the $7\sigma^2$ and $2\pi^4$ monomer orbitals, while the unoccupied dimer orbitals ($10b_u 3a_u 3b_g 10a_g$), ($11a_g 11b_u$), and ($12b_u 4a_u 12a_g 4b_g$) relate to the 3π, 8σ, and 4π monomer orbitals, respectively. The ground state geometry for the $(N_2O)_2$ dimer was calculated with MP2 perturbation theory using the 6-311+G(d) basis set. The distance between the two monomer centers of mass was calculated to be 348 pm which is in good agreement with the latest experimental value of 342.3 pm [40].

The optimized geometry was then used as input for TDDFT calculations of excited state wavefunctions and vertical excitation energies. In order to assess the influence of different functionals and basis sets, for the excited state calculations we have used B3LYP, MPW1PW91, and M052X functionals with different basis sets. In particular, the M052X functional was employed because it is known to be best suited for the description of non-covalent interactions such as the intermolecular forces forming the $(N_2O)_2$ dimer from the two N_2O molecules [49].

Table 1 lists the results for the excited state calculations for the N_2O monomer together with experimental results and previous assignments. While calculations were performed for singlet and for triplet states, only singlet states are considered here because they describe the experimentally observed absorption spectrum very well. The overall agreement between our TDDFT results, the theoretical results of Hopper [31] and the experimental values [24] is good, with the M052X functional yielding the least precise results for the monomer excited states, as expected. Generally, the TDDFT calculations tend to result in slightly too large values for vertical excitation energies. In Fig. 1 we present an overview over the experimental one-photon absorption spectrum of nitrous oxide taken from Ref. [24], together with theoretical transition energies from our own and from Hopper's [31] calculations.

The issue of assigning the onset of the very strong one-photon Rydberg excitation at 10.53 eV (84937 cm^{-1}) has been discussed controversially. Szarka and Wallace assigned it to the $3p\sigma^1\Pi$ ($^1_0 3$) $\leftarrow X^1\Sigma^+(^0_0 0)$ transition carrying one quantum of antisymmetric stretch in the electronically excited state [42]. Consequently, they identified an absorption feature at 10.31 eV (83188 cm^{-1}) as the corresponding band origin which is absent in Fig. 1, but strong in multi-photon excitation studies. Later, Cossart-Magos et al. reassigned the weak absorption feature at 10.31 eV as the origin of the one-photon forbidden $3p\pi^1\Delta \leftarrow X^1\Sigma^+$ transition and proposed the strong peak at 10.53 eV to be the origin of the $3p\sigma^1\Pi \leftarrow X^1\Sigma^+$ transition [28]. Both assignments are in accord with photoelectron spectroscopy (PES) experiments by Scheper et al. [44] who have identified the 10.31 eV feature as a band origin, but, unfortunately, did not report PES data for the strong absorption at 10.53 eV. Peak intensity arguments are not helpful to resolve this issue either, taking into account the drastically different intensities for one-, two-, and three-photon absorption schemes and the Jahn-Teller effect

Table 1
N_2O monomer excited singlet states and vertical excitation energies (energies in eV).

State	B3LYP[a]	MPW1PW91[a]	M052X[a]	Ref. [31]	Experimental data
M1 [$A^1\Sigma^+$]	6.48	6.50	5.68	7.59	6.3–7.6 [24]
M2,M3 [$B^1\Delta$]	6.82	6.90	6.88	7.65	6.3–7.6 [24]
M4,M5 [$C^1\Pi$]	8.32	8.53	8.82	8.35	8.1–8.8 [24]
M6 [$D^1\Sigma^+$]	10.02	10.19	10.53	10.11	9.2–10.0 [24]
M7,M8 [$^1\Pi(2\pi^3 3p\sigma)$]	10.87	11.07	11.18	10.2–10.4	10.53 [28]
M9–M11 [$^1\Sigma^-/^1\Delta(2\pi^3 3p\pi)$]	10.89–10.92	11.11–11.15	11.90–11.91	10.2–10.4	10.31 [28]

[a] This work (6-311+G(d) basis set).

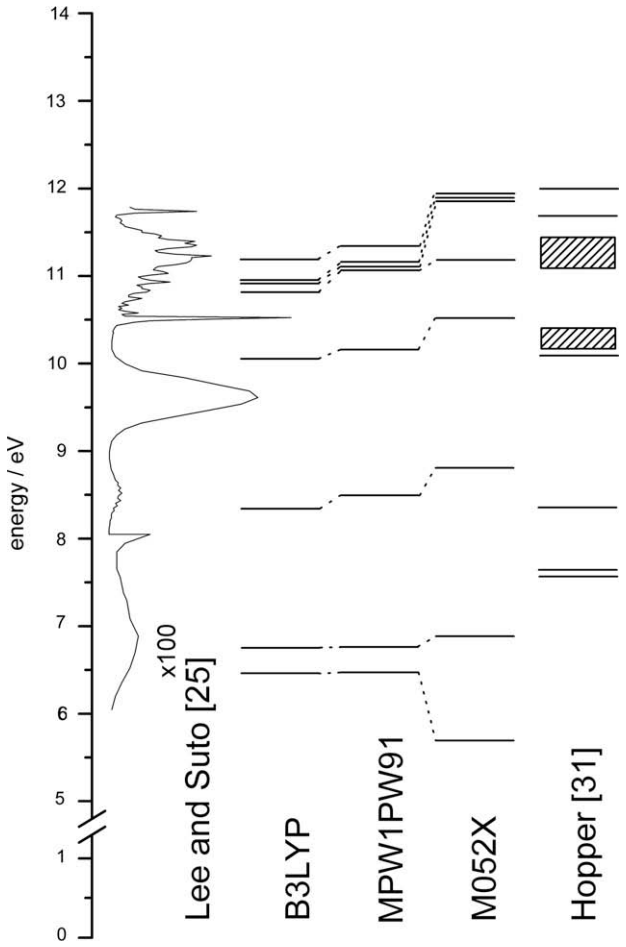

Fig. 1. Left column: N_2O one-photon absorption spectrum from Ref. [28]. Middle columns: vertical excitation energies of the N_2O monomer, calculated with different functionals (6-311+G(d) basis set). Right column: calculated vertical excitation energies of the N_2O monomer from Ref. [31].

Table 2
$(N_2O)_2$ dimer vertical excitation energies (6-311+G(d) basis set, energies in eV).

B3LYP		M052X	
State	Energy	State	Energy
D1,D2	6.31	D1,D2	5.42
D3–D6	6.67	D3–D6	6.69
D7–D14	7.67–7.73	D7–D10	8.80–8.83
D15–D18	8.28–8.32	D11–D18	9.58–9.65
D19–D22	9.38–9.49	D19	10.30
D23	10.09	D20	10.46
D24	10.21	D21–D26	10.98–11.05
D25–D26	10.66	D27,D28	11.19–11.23
D27–D30	10.68–10.72	D29,D30	11.71–11.72

contributing to increasing the complexity of excited state electronic structure.

With exception of the less precise M052X functionals, our own calculations predict both transitions, $3p\pi^1\Delta \leftarrow X^1\Sigma^+$ and $3p\sigma^1\Pi \leftarrow X^1\Sigma^+$, to occur very close to each other, i.e. with energetic separation of less than 0.1 eV. Although all calculations performed by us predict the $3p\pi^1\Delta \leftarrow X^1\Sigma^+$ transition to occur at slightly higher energies than the $3p\sigma^1\Pi \leftarrow X^1\Sigma^+$ transition, the separation in vertical excitation energies lies within the uncertainty of the calculations, such that we cannot prove the correctness of either previous assignment. In the following we have adopted the more recent assignment of Cossart-Magos et al. [28]. In any case, our predictions for the spectroscopic characteristics of the $(N_2O)_2$ dimer remain unaffected from a possible reassignment of the electronic monomer transitions in this region.

The 30 lowest dimer singlet states calculated with B3LYP and M052X functionals with 6-311+G(d) basis sets are listed in Table 2. Again, triplet states are not shown here because they were found to be of no significance for the monomer electronic transitions. For the M052X functional which is expected to yield the best results with respect to effects resulting from non-covalent interaction, dimer states D1–D6 and D11–D20 are essentially linear combinations of electronic excitation from the $(9b_u^2 2b_g^2 9a_g^2 2a_u^2)$ manifold into the $(10b_u 3a_u 3b_g 10a_g)$ manifold, while dimer states D7–D10 reflect excitation from the $(9b_u^2 2b_g^2 9a_g^2 2a_u^2)$ manifold into the $(11a_g 11b_u)$ manifold. Corresponding monomer transitions are $2\pi \rightarrow 3\pi$ and $2\pi \rightarrow 8\sigma$, respectively. Dimer states D21–D28 bear a significant contribution from excitation from the $(8b_u^2 8a_g^2)$ dimer orbitals (7σ monomer orbital) and states D29 and 30 mark the onset of excitation into the $(12b_u 4a_u 12a_g 4b_g)$ dimer orbitals, corresponding to the 4π monomer orbital. The transition into the dimer state D20 exhibits the largest oscillator strengths of all transitions calculated. The corresponding monomer state is M6 which agrees very well with the experimental one-photon absorption spectrum. Prominent dimer states are therefore D1, D7, D20, D21, and D29 which closely relate to the corresponding monomer states M1, M4, M6, M7, and M9. Comparing the excitation energies for those states, one finds that transitions into dimer electronically excited states generally appear near the transitions into the corresponding monomer states, with excitation energies lowered by 0.1–0.2 eV. In addition, several dimer states with no corresponding monomer states arise mainly due to the interaction of the monomer 2π and 3π orbitals in the dimer. Analyzing the B3LYP data yields very similar results.

From our calculations we expect the occurrence of dimer absorption features at the corresponding monomer transition wavelengths shifted to the red by 0.1–0.2 eV. The most promising candidate for observing dimer absorption in the ultraviolet is therefore the energy range just below the strong, sharp Rydberg peak at 10.53 eV. First, other than the absorption features at lower energies, this region is known to allow REMPI detection of the N_2O monomer [42,43]. Second, monomer transitions to the red of the prominent peak at 10.53 eV are weak and have a relatively narrow width ca. 100 cm^{-1} at room temperature, which is small enough to allow for sufficiently large spectral regions free from possibly interfering monomer absorption. Additionally, it can be expected that the absorption bandwidth will be even smaller at the low temperatures of a supersonic expansion.

4. Experimental results

Based on the results of our calculations, we have performed measurements at excitation energies between 10.15 and 10.55 eV (82 000 cm^{-1} and 85 000 cm^{-1}). The upper trace in Fig. 2 displays an overview over a room temperature spectrum, corresponding to two-photon excitation at wavelengths between 235.3 and 243.9 nm. N_2O was detected by (2 + 1) REMPI at fragment mass 30 (NO^+) via transitions belonging to the Rydberg series converging to the ionic ground state $X^2\Pi_\Omega$ of N_2O^+ at 103963 cm^{-1}. Main peaks are labeled with the corresponding transitions according to the assignment of Ref. [28]. The $3p\sigma^1\Pi \leftarrow X^1\Sigma^+$ band origin at 84 937 cm^{-1} which is the dominant feature in the one-photon absorption spectrum appears with moderate intensity in the (2 + 1)-REMPI spectrum. Where bending vibrations occur, those Renner-Teller sub-states which were observed in the spectrum are assigned. Signals recorded at mass 28 (N_2^+) yielded identical spectra at much lower intensities, with the exception of the weak

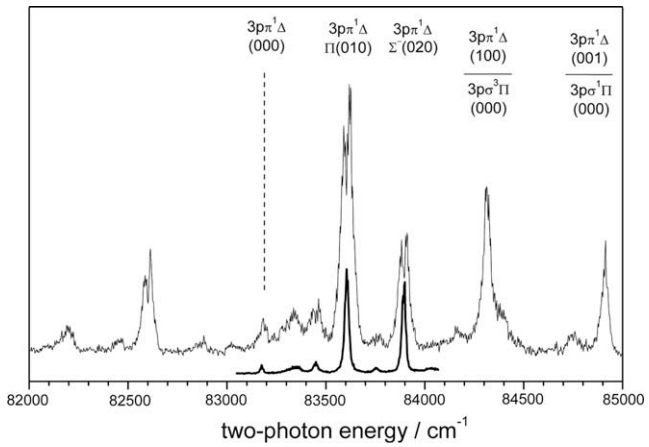

Fig. 2. Upper trace: room temperature spectrum recorded at mass 30. Assignments are made according to Ref. [28]. Lower trace: jet-cooled spectrum around the band origin.

double shoulder at 84400 and 84450 cm^{-1} which accidentally occurs in this wavelength range and belongs to three-photon resonant transitions into a Rydberg state converging to the ionic B state of N_2O^+ [42]. The $3p\pi\,^1\Delta$ band origin at 83188 cm^{-1} which was suggested to be the origin of the $3p\sigma\,^1\Pi$ band by Szarka et al. [42] can only weakly be seen in the (2 + 1)-REMPI spectra, in striking contrast to three-photon excitation. At higher excitation energies several stronger transitions into vibrationally excited levels of the $^1\Delta$ Rydberg state are observed complemented by bending mode hot bands on the red side of the band origin. While vibrational bands cannot rotationally be resolved due to fast predissociation of the Rydberg state, rotational excitation is evidenced by several of the band shapes.

The lower trace in Fig. 2 shows the spectrum monitored for a jet-cooled sample from the $3p\pi\,^1\Delta \leftarrow\leftarrow X\,^1\Sigma^+$ band origin to the strong transitions into the Renner-Teller sub-states of the vibrationally excited bending mode of the $^1\Delta$ Rydberg state.

In order to monitor the $(N_2O)_2$ dimer we have scanned the spectral range displayed in Fig. 2 for different nozzle expansion conditions. Fig. 3 shows the spectral region to the red of the $^1\Pi$ state

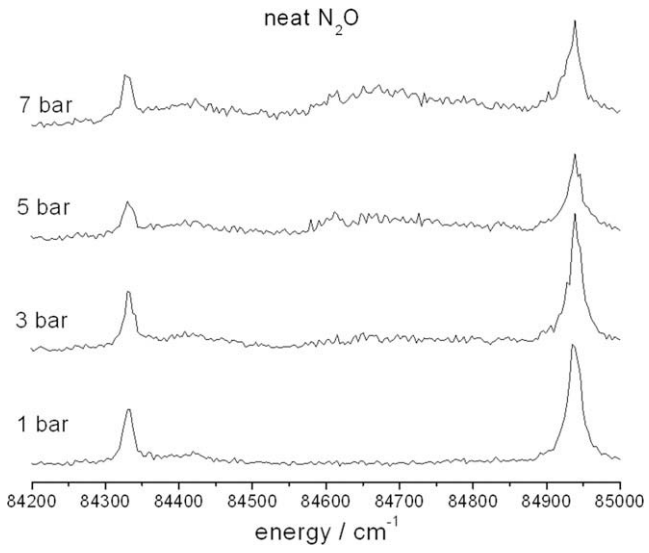

Fig. 3. Complex formation in dependence on nozzle stagnation pressure, evidenced by a broad spectral feature at 84650 cm^{-1} between monomer peaks at 84330 cm^{-1} and at 84937 cm^{-1}.

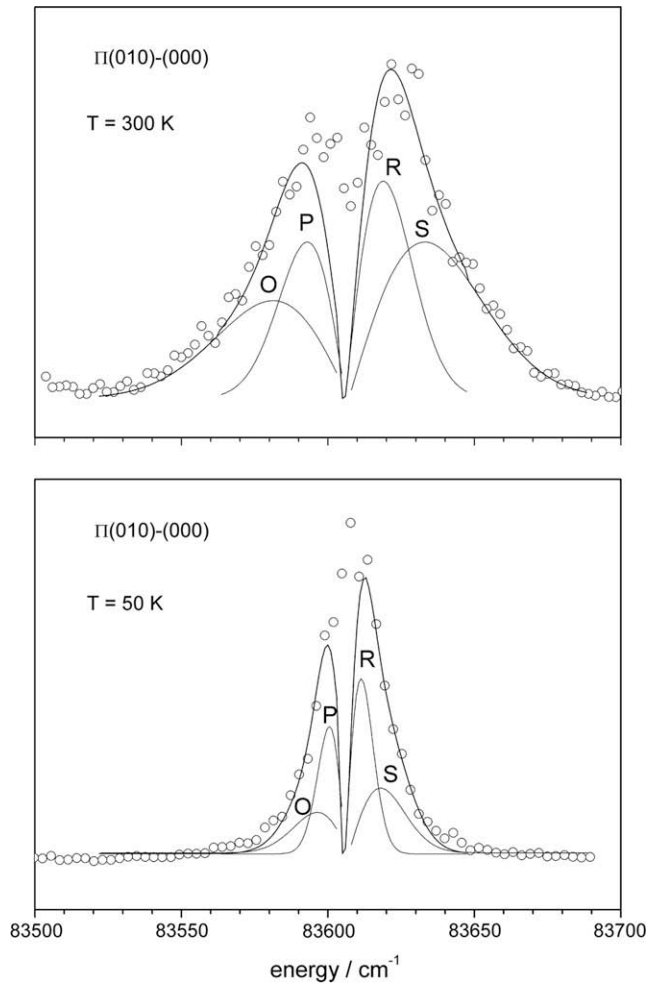

Fig. 4. Superposition of rotational branches O, P, R, and S (solid lines) for temperatures of 300 K (upper panel) and 50 K (lower panel). Simulated data agree very well with measured data (open circles) for bulk (upper panel) and beam (lower panel) conditions.

band origin. Traces represent spectra obtained for different stagnation pressures between 1 and 7 bar for neat N_2O samples. For stagnation pressures larger than 2 bar, a broad new feature rises at 84650 cm^{-1}, between the two prominent monomer peaks at 84330 and 84937 cm^{-1}.

5. Discussion

At low temperatures, the envelopes of the rotational branches seen at room temperature collapse into a single narrow peak (cf. Fig. 2). The $\Pi(010)$–(000) transition can be used as a temperature probe as is demonstrated in Fig. 4. In the upper panel of Fig. 4, the band is approximated by a set of four rotational branches O, P, R, and S which have been simulated for room temperature in the rigid rotor approximation with identical rotational constants B_0 = 0.418 cm^{-1} for initial and final states [50]. The Q branch has not been considered because in this approximation its influence on the wings of the band shape is negligible. The use of equal rotational constants for initial and final states is justified by the nearly symmetric shape of the band and because the rotational constant for the N_2O^+ ion is very similar to the one of the neutral molecule [51–53]. In view of the significant simplification inherent in this approach, the agreement between the approximation and the experimentally observed band shape is more than satisfactory. Using this basic calibration procedure, in the lower panel of

Fig. 4 a temperature of ca. 50 K was estimated in the same way for the temperature of the jet-cooled pure N_2O sample.

Given the temperature in the molecular beam, it is reasonable to assign the new absorption features shown in Fig. 3 to a $(N_2O)_n$ van der Waals complex with $n \geqslant 2$. Our calculations predict dimer absorption ca. 0.1–0.2 eV below the corresponding monomer absorption. The wavelength of the experimentally observed dimer absorption agrees well with the predicted relative position of the dimer excited states 29 and 30 in Table 2 with respect to the 4sσ Rydberg excitation of the monomer. These dimer excited states are mainly contributed to by linear combinations of electronic excitation from the $9b_u2b_g9a_g2a_u$ manifold into the $11b_u$ and the $4a_u$ orbitals. Wavefunctions with a_u symmetry can only be composed from π monomer wavefunctions. Therefore the excitation into the $4a_u$ dimer orbital corresponds to the 3pπ Rydberg excitation in the monomer. Similarly, the excitation into the $11b_u$ dimer orbital corresponds to the 4sσ Rydberg excitation in the monomer.

To the best of our knowledge, this is the first detection of N_2O van der Waals complexes ever reported for the ultraviolet wavelength range. Unfortunately, a direct determination of the complex mass is not feasible by the employed UV excitation scheme, since under the employed experimental conditions even the monomer undergoes almost complete fragmentation in the TOF spectrometer as has also been observed previously [42,43].

For the spectra shown in Fig. 3 which were obtained under variation of the nozzle stagnation pressure a threshold behavior was observed, i.e. there exists a minimum stagnation pressure needed in order for the effect to occur. This threshold behavior is likely to result from the need of sufficiently many three-body collisions during the expansion through the nozzle in order to energetically stabilize a newly associated $(N_2O)_2$ dimer. Above this threshold value, no new absorption features have been observed in the wavelength range under consideration while intensities prove that the dimer concentration correlates with stagnation pressure. Therefore, we propose a "core" complex to be responsible for the new spectral feature which is likely to be the $(N_2O)_2$ dimer. Nevertheless, the formation of larger complexes cannot be ruled out based on the spectroscopic information contained in the observed spectral features. The intensity decrease of the monomer peaks for expansions at higher stagnation pressures can be understood by the increase in the degree of complexation with rising pressure, going along with a decrease in monomer concentration, as it was also observed, e.g., for HI–Xe complexes [54].

A similar effect has only recently been observed for $NO{\cdot}Ar_n$ complexes [45,46]. There, it was found that for $n > 2$ the spectral signature of the complex remains essentially unchanged from the $n = 2$ case, which was interpreted as being evidence of a "core" $NO{\cdot}Ar_2$ complex. Argon particles forming an outer shell around the core complex do not noticeably affect the Rydberg electron which is effectively shielded by the first two argon atoms. A similar mechanism might be active for the N_2O molecule, in accordance with the independence of the shapes of the new spectral features from the sample composition.

The possibility to detect $(N_2O)_n$ complexes by (2 + 1)-REMPI in the ultraviolet has an important consequence for the study of the bimolecular reaction (1). This reaction can easily be photoinitiated in a pure sample of N_2O by 193 nm photolysis of N_2O:

$$N_2O + h\nu(\lambda = 193\ \text{nm}) \rightarrow N_2 + O(^1D), \quad (2)$$

and products can easily be analyzed by REMPI detection of NO in combination with imaging techniques. Consequently, reaction (1) has received considerable attention in the past and continues doing so.

For the detailed analysis of reaction (stereo)dynamics, the reactants on the left side of reaction (1) need to be prepared in a well-defined manner which is why jet-cooling of the N_2O sample is popular and a sensible thing to do. However, complex formation of N_2O needs to be accounted for, particularly because the outcome of reaction (1) is known to be strongly influenced by the geometry constraint of the dimer configuration. Until now, complex formation could only be assessed by electron impact ionization [6,8] or from the analysis of the observed product data [19].

The advantage of the detection of N_2O complexes at 84650 cm^{-1} is that conditions under which reaction (1) is being studied can be characterized by the same detection technique used to study the reaction itself. Thus, expansion conditions can be controlled such that initiating the reaction from within a cluster will be preferred or suppressed, allowing to obtain new insight into the dynamics of the reaction by defining the reaction geometry.

6. Conclusion

(2 + 1)-REMPI detection of N_2O between 82000 cm^{-1} and 85000 cm^{-1} is demonstrated for room temperature and for jet-cooled N_2O samples. A temperature of ca. 50 K is achieved in the jet expansion of neat N_2O. Formation of N_2O van der Waals complexes occurs for high stagnation pressure jet expansions in pure N_2O. For the first time, $(N_2O)_n$ van der Waals complexes have spectroscopically been detected by (2 + 1)-REMPI in the ultraviolet, opening the possibility for characterization and control of bimolecular reactions photoinitiated in N_2O containing samples. Calculations using time-dependent density function theory accurately reproduce the monomer absorption properties and suggest the $(N_2O)_2$ dimer to be a major species responsible for high stagnation pressure absorption features.

Acknowledgments

Acquiring room temperature data was skillfully assisted by Benjamin Ames within an undergraduate exchange program between the University of Utah and Technische Universität Braunschweig, sponsored by the German Academic Exchange Service (DAAD). A.R. gratefully acknowledges financial assistance of the Alexander von Humboldt foundation.

References

[1] J.N. Galloway, A.R. Townsend, J.W. Erisman, M. Bekunda, Z. Cai, J.R. Freeney, L.A. Martinelli, S.P. Seitzinger, M.A. Sutton, Science 320 (2008) 889.
[2] R.A. Duce, J. LaRoche, K. Altieri, K.R. Arrigo, A.R. Baker, D.G. Capone, S. Cornell, F. Dentener, J. Galloway, R.S. Ganeshram, R.J. Geider, T. Jickells, M.M. Kuypers, R. Langlois, P.S. Liss, S.M. Liu, J.J. Middelburg, C.M. Moore, S. Nickovic, A. Oschlies, T. Pedersen, J. Prospero, R. Schlitzer, S. Seitzinger, L.L. Sorensen, M. Uematsu, O. Ulloa, M. Voss, B. Ward, L. Zamora, Science 320 (2008) 893.
[3] S. Solomon et al., in: S. Solomon et al. (Eds.), Climate Change 2007: The Physical Science Basis, Cambridge University Press, Cambridge, 2007.
[4] H. Okabe, Photochemistry of Small Molecules, Wiley Interscience, New York, 1978.
[5] T.E. Gough, R.E. Miller, G. Scoles, J. Chem. Phys. 69 (1978) 1588.
[6] N. Goldstein, G.D. Greenblatt, D.R. Wiesenfeld, Chem. Phys. Lett. 83 (1983) 21.
[7] K. Honma, O. Kajimoto, Chem. Phys. Lett. 117 (1985) 123.
[8] K. Honma, Y. Fujimura, O. Kajimoto, G. Inoue, J. Chem. Phys. 88 (1988) 4739.
[9] F. Green, G. Hancock, A.J. Orr-Ewing, M. Brouard, S.P. Duxon, P.A. Enriquez, R. Sayos, J.P. Simons, Chem. Phys. Lett. 182 (1991) 568.
[10] M. Brouard, S.P. Duxon, A. Enriquez, R. Sayos, J.P. Simons, J. Phys. Chem. 95 (1991) 8169.
[11] M. Brouard, S.P. Duxon, A. Enriquez, J.P. Simons, J. Chem. Phys. 97 (1992) 741.
[12] X.B. Wang, H.Z. Li, Q.H. Zhu, F.N. Kong, H.G. Yu, J. Chin. Chem. Soc. 42 (1995) 399.
[13] H. Akagi, Y. Fujimura, O. Kajimoto, J. Chem. Soc. Faraday Trans. 94 (1998) 1575.
[14] H. Tsurumaki, Y. Fujimura, O. Kajimoto, J. Chem. Phys. 111 (1999) 592.
[15] H. Akagi, Y. Fujimura, O. Kajimoto, J. Chem. Phys. 111 (1999) 115.
[16] P.J. Pisano, M.S. Westley, P.L. Houston, Chem. Phys. Lett. 318 (2000) 385.
[17] G. Hancock, V. Haverd, Phys. Chem. Chem. Phys. 5 (2003) 2369.

[18] S. Kawai, Y. Fujimura, O. Kajimoto, T. Takayanagi, J. Chem. Phys. 120 (2004) 6430.
[19] N. Gödecke, 3D Velocity Mapping: Vollständige Charakterisierung der bimolekularen Reaktion $O(^1D) + N_2O \rightarrow NO + NO$, Cuvillier, Göttingen, 2008.
[20] N. Gödecke, S. Kauczok, A.I. Chichinin, C. Maul, K.-H. Gericke, J. Chem. Phys. (submitted for publication).
[21] A.B.F. Duncan, J. Chem. Phys. 4 (1936) 638.
[22] M. Zelikoff, K. Watanabe, E.C.Y. Inn, J. Chem. Phys. 21 (1953) 1643.
[23] Y. Tanaka, A.S. Jursa, F.J. Leblanc, J. Chem. Phys. 32 (1960) 1205.
[24] R.H. Huebner, R.J. Celotta, S.R. Mielczarek, C.E. Kuyatt, J. Chem. Phys. 63 (1975) 4490–4494.
[25] L.C. Lee, M. Suto, J. Chem. Phys. 80 (1984) 4718–4726.
[26] W.F. Chan, G. Cooper, C.E. Brion, Chem. Phys. 180 (1994) 77–88.
[27] J.B. Nee, J.C. Yang, P.C. Lee, X.Y. Wang, C.T. Kuo, Chin. J. Phys. 37 (1999) 172–180.
[28] C. Cossart-Magos, M. Jungen, F. Launay, J. Chem. Phys. 114 (2001) 7368.
[29] A.M. Velasco, E. Bustos, I. Martin, C. Lavin, Int. J. Quantum Chem. 84 (2001) 70.
[30] M. Noh Daud, G.G. Balint-Kurti, A. Brown, J. Chem. Phys. 122 (2005) 054305.
[31] D.G. Hopper, J. Chem. Phys. 80 (1984) 4290–4316.
[32] O. Echt, M. Knapp, K. Sattler, E. Recknagel, Z. Phys. B 53 (1983) 71.
[33] R.E. Miller, R.O. Watts, A. Ding, Chem. Phys. 83 (1984) 155.
[34] Y. Ohshima, Y. Matsumoto, M. Takami, K. Kuchitsu, Chem. Phys. Lett. 152 (1988) 294.
[35] H.-B. Qian, W.A. Herrebout, B.J. Howard, Mol. Phys. 91 (1997) 689.
[36] Z.S. Huang, R.E. Miller, J. Chem. Phys. 89 (1988) 5408.
[37] R.E. Miller, R.O. Watts, Chem. Phys. Lett. 105 (1984) 409.
[38] A. Hecker, I. Scheele, M. Havenith, Phys. Chem. Chem. Phys. 5 (2003) 2333.
[39] A. Hecker, Ph.D. Thesis, Ruhr-Universität Bochum, Bochum, Germany, 2003.
[40] M. Dehghani, M. Afshari, Z. Abusara, N. Moazzen-Ahmadi, A.R.W. McKellar, J. Chem. Phys. 126 (2007) 164310.
[41] M. Dehghani, M. Afshari, Z. Abusara, C. van Eck, N. Moazzen-Ahmadi, J. Mol. Spectrosc. 247 (2008) 123.
[42] M.G. Szarka, S.C. Wallace, J. Chem. Phys. 95 (1991) 2336.
[43] E. Patsilinakou, R.T. Wiedemann, C. Fotakis, E.R. Grant, J. Chem. Phys. 91 (1989) 3916.
[44] C.R. Scheper, J. Kuijt, W.J. Buma, C.A. de Lange, J. Chem. Phys. 109 (1998) 7844.
[45] D.E. Bergeron, A. Musgrave, V.L. Ayles, R.T. Gammon, J.A.E. Silber, T.G. Wright, J. Chem. Phys. 125 (2006) 144319.
[46] D.E. Bergeron, A. Musgrave, R.T. Gammon, V.L. Ayles, J.A.E. Silber, T.G. Wright, B. Wen, H. Meyer, J. Chem. Phys. 124 (2006) 214302.
[47] Gaussian 03, Revision E.01, M.J. Frisch, G.W. Trucks, H.B. Schlegel, G.E. Scuseria, M.A. Robb, J.R. Cheeseman, J.A. Montgomery, Jr., T. Vreven, K.N. Kudin, J.C. Burant, J.M. Millam, S.S. Iyengar, J. Tomasi, V. Barone, B. Mennucci, M. Cossi, G. Scalmani, N. Rega, G.A. Petersson, H. Nakatsuji, M. Hada, M. Ehara, K. Toyota, R. Fukuda, J. Hasegawa, M. Ishida, T. Nakajima, Y. Honda, O. Kitao, H. Nakai, M. Klene, X. Li, J.E. Knox, H.P. Hratchian, J.B. Cross, V. Bakken, C. Adamo, J. Jaramillo, R. Gomperts, R.E. Stratmann, O. Yazyev, A.J. Austin, R. Cammi, C. Pomelli, J.W. Ochterski, P.Y. Ayala, K. Morokuma, G.A. Voth, P. Salvador, J.J. Dannenberg, V.G. Zakrzewski, S. Dapprich, A.D. Daniels, M.C. Strain, O. Farkas, D.K. Malick, A.D. Rabuck, K. Raghavachari, J.B. Foresman, J.V. Ortiz, Q. Cui, A. G. Baboul, S. Clifford, J. Cioslowski, B.B. Stefanov, G. Liu, A. Liashenko, P. Piskorz, I. Komaromi, R.L. Martin, D.J. Fox, T. Keith, M.A. Al-Laham, C.Y. Peng, A. Nanayakkara, M. Challacombe, P.M.W. Gill, B. Johnson, W. Chen, M.W. Wong, C. Gonzalez, J.A. Pople, Gaussian, Inc., Wallingford CT, 2004.
[48] C. Maul, T. Haas, K.-H. Gericke, F.J. Comes, J. Chem. Phys. 102 (1995) 3238.
[49] Y. Zhao, N.E. Schultz, D.G. Truhlar, J. Chem. Theory Comput. 2 (2006) 364.
[50] B.A. Andreev, A.V. Burenin, E.N. Karyakin, A.F. Krupnov, S.M. Shchapin, J. Mol. Spectrosc. 62 (1976) 125.
[51] J.H. Callomon, F. Creutzberg, Phil. Trans. R. Soc. A 277 (1974) 157.
[52] H. Gritli, Z. Ben Lakhdar, G. Chambaud, P. Rosmus, Chem. Phys. Lett. 178 (1993) 223.
[53] M. Larzillière, C. Jungen, Mol. Phys. 67 (1989) 807.
[54] M.O. Bulanin, A.V. Domanskaya, K. Kerl, C. Maul, Mol. Phys. 104 (2006) 2685.